

Self-Tuning PID Control for a Continuous Dense Phase System

Valeria T. Myers¹, Luis F. Recalde²

¹ Department of Control (Electrical) Systems, University of Wisconsin-Platteville, 1 University Plaza, Wisconsin, 53818, USA
E-mail: recaldev@uwplatt.edu

² Universidad de las Fuerzas Armadas ESPE, Quijano y Ordóñez, Latacunga, 050150, Ecuador
E-mail: lfrecale1@espe.edu.ec

Abstract— This paper proposes a Self-Tuning PID controller for continuous dense phase (CDP) conveying systems, which are applied in the industry e.g., the transportation of pet food where the shape of the final product is important. CDP systems are subject to parametric changes and external disturbances where online system identification is the best choice for startup tuning. Moreover, for this controller the mathematical model was developed considering that a total flow is calculated accounting the flow needed to transport the material at the desired convey velocity, plus the flow losses (airlock leakage flow, and future flow losses for wear). Additionally, the mathematical model is used to develop a self-tuning PID controller, which will keep a main flow rate of the system based on the convey velocity set-point. Likewise, the controller will regulate the aperture of a valve to allow only the necessary air pass to form the slugs in a dense phase system. Furthermore, the coefficients of the mathematical model to fit a real system are estimated using Recursive Least Squares method. Finally, simulation tests are carried out to validate the proper functioning of the controller.

Keywords— PID controller; continuous dense phase system; airlock leakage; recursive least squares.

I. INTRODUCTION

Pneumatic conveying system is defined as the transport of various granular solids and dry powders using an air stream as a transportation media [1]. Recent developments shows the great advantages this type of system offers to factories, for that reason in the last years pneumatic system are chosen over mechanical transports. Some of the candidate industries for this type of transport are the following: agriculture, mining, chemical, pharmaceutical, paint manufacturing, food and metal refining and processing[2].

The pneumatic conveying systems can be classified based on the average particle concentration in the pipe and the air velocity:(1) dilute phase system where the mass flow ratio of 0-15 and high velocity; and (3) dense phase where flow ratio greater than 15 and low velocity[3].

The benefits of dense phase conveying over mechanical conveying are noticeably endless .The number one reason to apply this kind of system is when the product being handled is highly friable[4]. All the benefits are : (1) Low air energy consumption; (2) Minimal material degradation; (3) Minimal material segregation; (4) Low pipeline and component wear; (5) Fewer maintenance points; (6) Capable of handling abrasive materials; (7) Capable of handling

fragile materials; (8) Environmentally friendly; no material spillage, no dust emission, low noise emission; (9) Flexibility in routing; and (10) Ease of automation and control [3]

Because the dense phase pneumatic conveying moves the material in the pipe at low velocity, the particles of this material begin to fall to the bottom of the pipe. The technical term used to describe the velocity at which particles fall from airstream suspension is "saltation velocity". Consequently, the main goal of a dense phase conveying system is to slow down the velocity of the product in the pipe. At low velocities, the product lies down for periods of time in the bottom of a horizontal line and it is blown under pressure to the discharge point in slug or plug shapes.

Unfortunately, there is not enough research about dense phase systems, although the interest from factories is growing. Until now most of the designs of this type of system is purely mechanical, making this design highly sensitive to system disturbances and parametric changes that may arise. The implementation of feedback control to operate at low air flow rates without compromising reliability it becomes necessary.

Dense phase has so far not been successfully modelled in a way that would make those models applicable to classical control design[1], [5]; consequently, other investigations [1] suggest intelligent controllers to stabilize this kind of system using Artificial Neural Networks.

Hence, this paper proposes a self-tuning PID controller to solve the problem of parametric changes and disturbances in this system. This controller is based on online estimation of discrete data of a system applying recursive least squares programming method[6], [7]. Finally, using the pole placement method the parameters of the controller are adjusted to give the desired control performance even if the parameters of the system changed.

This paper is divided into six sections, including the introduction. In section 2 the problem structure, the mathematical model and the validation of the system are presented. The design of the controller is presented in section 3. The results and discussions are shown in section 4. Finally the conclusions are presented in section 5.

II. SYSTEM STRUCTURE

A. Problem Structure

Many different modes of dense phase conveying have been developed to take advantage of the different properties and characteristics of bulk solid used in industry [5]. The actual methods for dense phase conveying systems control the airflow or pressure based on mechanical calculations, which require precise parameters. Consequently, the actual methods require a lot of testing to determine the value of the parameters. This paper proposes to use a similar concept of Fig.1 to control the supply airflow within the convey piping, with the incorporation of an advanced airflow controller

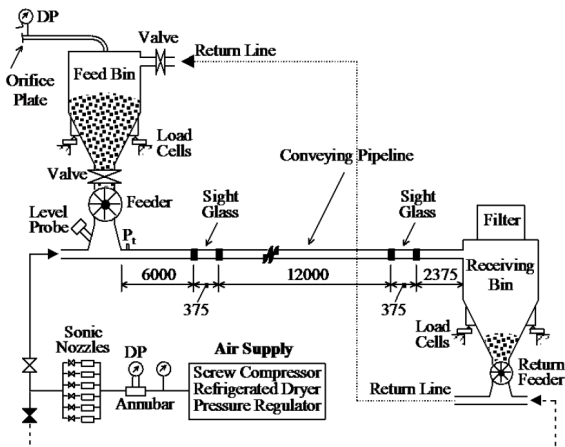


Fig. 1 Full-scale test ring to measure air leakage [4]

B. Mathematical Model of Continuous Dense Phase System

This paper analyzes a continuous dense phase system which is configured for the air supply provided by a blower, a valve to control the air flow going to the convey pipe, a rotatory valve which feeds the line, and the instrumentation to measure the airflow and pressures.

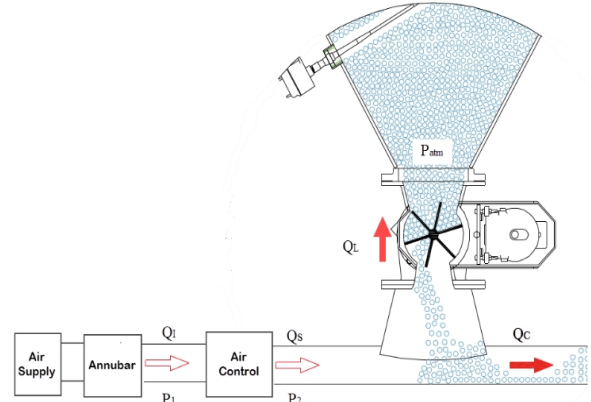


Fig. 2 A sample line graph using colors which contrast well both on screen and on a black-and-white hardcopy

The drop in pressure across the orifice in the valve is used to measure the air flowrate Q_s . There are many equations to calculate the flow rate in a valve, but the best approximation of a real curve was found with the Bernoulli's equation (air speed is subsonic).

$$\dot{Q}_s(t) = \frac{A_v(t) \zeta_3 \chi_1 \chi_2}{\zeta_1 \sqrt{1 - \left(\frac{A_v(t) \chi_2}{\zeta_1 A_p}\right)^2}} \sqrt{\frac{\zeta_2 R(P_1(t) - P_2(t))}{P_2(t) + P_{atm}}} T_1 \quad (1)$$

where T_1 is a factor that allows the transformation of actual flow to a standard flow.

$$T_1 = \frac{P_2(t) + P_{atm}}{P_{std}}$$

The initial air flowrate Q_1 is based on the blower speed[8]. Q_s is equal to Q_1 when they are calculated in standard volumetric flow and from this equality P_2 can be found.

$$\dot{P}_2(t) = \frac{P_1(t) \sigma_4 + P_{atm} \sigma_4 - \sigma_1 + \sigma_3}{\sigma_2} \quad (2)$$

where:

$$\sigma_1 = A_p A_v(t) \zeta_1 \zeta_2 \zeta_3 P_{atm}^2 R T_s \chi_3 \chi_4$$

$$\sigma_2 = 2 A_p A_v(t) \zeta_1 \zeta_2 \zeta_3 P_{atm} R T_s \chi_5 \chi_6$$

$$\sigma_3 = A_p A_v(t) \zeta_1 \zeta_2 \zeta_3 P_1(t) P_{atm} R T_s \chi_7 \chi_8$$

$$\sigma_4 = \sqrt{\zeta_2 P_{atm} R T_s (4 A_v(t)^2 N^2 P_{atm} RPM_{max}^2 T_s \chi_9^2 \chi_{10}^2 \dots)}$$

$$\dots - 4 A_p^2 \zeta_1^2 N(t)^2 P_{atm} RPM_{max}^2 T_s \chi_{11}^2 \dots$$

$$\dots - 4 A_p^2 \zeta_1^4 \zeta_2 P_1(t) P_{std} \chi_{12}^2 \chi_{13}^2 \dots$$

$$\dots 4 A_v(t)^2 \zeta_1^2 \zeta_2 P_1(t) P_{std} \chi_{14}^2 \chi_{15}^2 \chi_{16}^2 \dots$$

$$\dots 8 A_p^2 \zeta_1^3 N(t) P_{atm} RPM_{max} T_s \chi_{17}^2 \chi_{18} \sigma_5 \dots$$

$$\dots -8 A_v(t)^2 \zeta_1 N(t) P_{atm} RPM_{max} T_s \chi_{19}^2 \chi_{20}^2 \chi_{21} \sigma_5 \dots$$

$$\dots A_p^2 A_v(t)^2 \zeta_1^2 \zeta_2 \zeta_3^2 P_{atm} R T_s \chi_{22}^2 \chi_{23}^2$$

$$\sigma_5 = \sqrt{\frac{\zeta_2 P_1(t) P_{std}}{P_{atm} T_s}}$$

The equation to model the pressure before the air control valve P_1 was proposed based on the curve generates from the real values of the system.

$$\dot{P}_1(t) = N(t)^2 \chi_{24} + N(t) \chi_{25} + A_v(t) \chi_{26} \quad (3)$$

TABLE I
PARAMETERS OF DENSE PHASE SYSTEM

System	Parameter	Units
Q_s	Flow rate	Scfm
P_1	Pressure before control valve	$\frac{lb_f}{in^2}$
P_2	Pressure after control valve	$\frac{lb_f}{in^2}$
A_v	Control valve opening	%open
N	Blower speed	%rpm
ζ_1	Valve maximum open	%open
ζ_2	Average temperature	°F
ζ_3	Conversion Factor	
A_p	Pipe area	ft^2
R	Universal Gas Constant	$\frac{ft lb_f}{lb^o R}$
P_{atm}	Atmospheric Pressure	$\frac{lb_f}{in^2}$
P_{std}	Standard Pressure	$\frac{lb_f}{in^2}$
RPM_{max}	Maximum blower revolutions per minute	rpm
T_s	Standard Temperature	°R

Table 1 shows the variables used in this system with their respective units.

C. Mathematical Model Identification and Validation

The identification and validation of the mathematical model (1), (2) and (3) that represents the behavior of the Dense Phase System is tested in this section. The main objective is to determine the value $\chi = [\chi_1 \ \chi_2 \ \dots \ \chi_l]$ with $l=26$, which adjust the mathematical model with the real system. The differential equations (1), (2) and (3) are solved through Euler approximations (4), (5) and (6), where T_s is a

sample time and $k \in \{1, 2, 3, 4, 5, \dots\}$, in orden the system can be simulated and the control algorithms can be tested.

$$Q_s(k+1) = Q_s(k) + \dot{Q}_s(k) T_s \quad (4)$$

$$P_1(k+1) = P_1(k) + \dot{P}_1(k) T_s \quad (5)$$

$$P_2(k+1) = P_2(k) + \dot{P}_2(k) T_s \quad (6)$$

The identification of the dense phase system was carried out using optimization techniques, where an objective is to minimize a cost function (7), varying the values of the vector χ , where $\tilde{\mathbf{h}}(k) = [Q_{sr}(k) - Q_s(k) \ P_{1r}(k) - P_1(k) \ P_{2r}(k) - P_2]^T$ is the vector of errors between values of the real system and mathematical model, $Q_{sr}(k), P_{1r}(k), P_{2r}(k)$ are the values obtained from the real system finally \mathbf{Q} is positive definite diagonal matrix that will weigh the vector of errors [9].

$$\mathbf{J} = \sum_{n=k}^{k+1} \tilde{\mathbf{h}}(k)^T \mathbf{Q} \tilde{\mathbf{h}}(k) \quad (7)$$

subject to:

$$Q_s(k+1) = Q_s(k) + \dot{Q}_s(k) T_s$$

$$P_1(k+1) = P_1(k) + \dot{P}_1(k) T_s$$

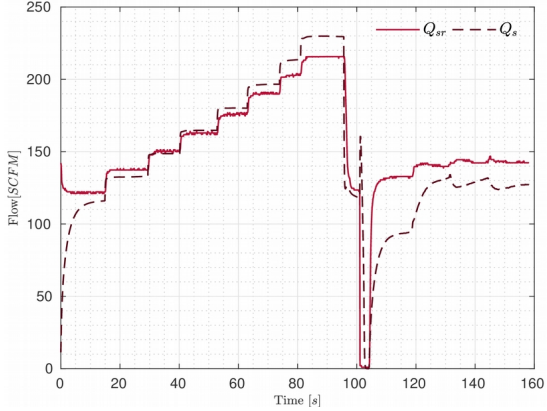
$$P_2(k+1) = P_2(k) + \dot{P}_2(k) T_s$$

The parameters of the Dense Phase System are presents in the Table 2.

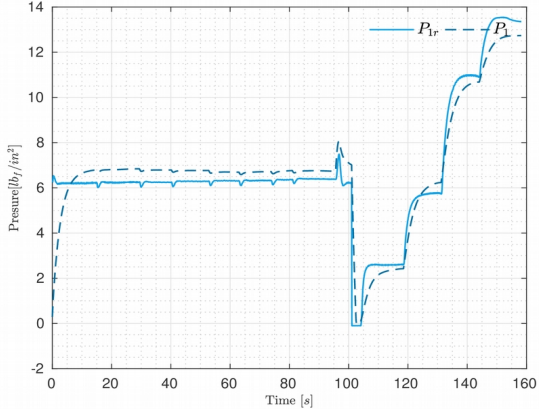
TABLE II
SYSTEM PARAMETERS OF DENSE PHASE SYSTEM

System	Parameters							
Flow System Q_s	χ_1	χ_2						
	2.59	0.013						
Pressure 2 P_2	χ_3	χ_4	χ_5	χ_6	χ_7	χ_8	χ_9	
	0.04	0.04	0.07	0.05	-0.03	-0.03	0.06	
	0.06	0.01	0.05	0.04	0.04	0.05	0.02	
	χ_{10}	χ_{11}	χ_{12}	χ_{13}	χ_{14}	χ_{15}	χ_{16}	
	0.02	0.008	0.03	0.03	0.18	0.18	0.04	
	χ_{17}	χ_{18}	χ_{19}	χ_{20}	χ_{21}	χ_{22}	χ_{23}	
Pressure 1 P_1	χ_{24}	χ_{25}	χ_{26}					
	0.02	0.2	0.06					

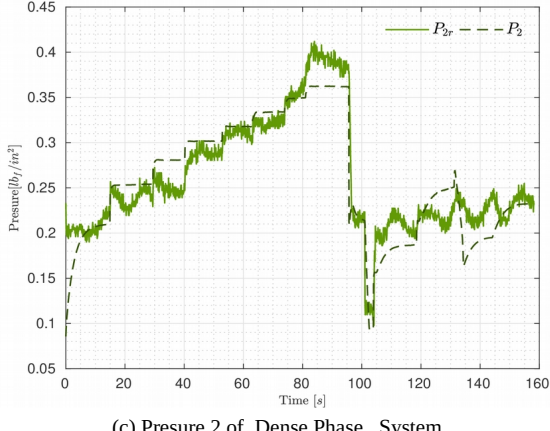
The experimental data for the validation procedures are shown in Fig. 3, where you can see the good performance of the proposed mathematical model.



(a) Flow rate of Dense Phase System



(b) Pressure 1 of Dense Phase System



(c) Pressure 2 of Dense Phase System
Fig. 3 Validation data of the proposed mathematical model of the Dense Phase System .

III. CONTROLLER DESIGN

The proposed control scheme shows in Fig 4, allows that the flow rate of the dense phase system $Q_s(k)$ track a desired flow $Q_{sd}(k)$ in order to generates the slugs of specific material. This effect is produced by making variations in the $Q_{sd}(k)$ with respect to $P_2(k)$, this produces a saw-tooth-shaped set point.

The control objective is achieved through a designed a control system, which comprises 2 stages: (1) a PID controller that allows $P_1(k)$ tracking the desired pressure $P_{1d}(k)$ through variations in Blower Speed $N(k)$, which makes the system stable, (2) self tuning PID controller, that

adjust the controller gains online achieving the smallest tracking error between $Q_{sd}(k)$ and $Q_s(k)$ through variations in control valve $A_v(k)$, this is achieved using recursive least squares and pole assignment methods.

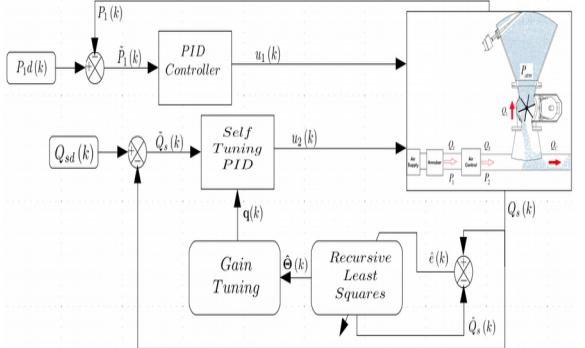


Fig. 4 Validation data of the proposed mathematical model of the Dense Phase System .

D. The PID controller for P_1

In real industrial applications, the recurrent algorithms are more suitable for practical use in this sense a PID controller with digital output can be applied [10] , where main objective is calculate the increment change $\Delta N(k)$, obtained the following equations (4), (5)

$$N(k)=\Delta N(k)+N(k-1) \quad (4)$$

$$\Delta N(k)=K_p(\tilde{P}_1(k)-\tilde{P}_1(k-1))+K_I(\tilde{P}_1(k)) \dots$$

$$\dots K_D(\tilde{P}_1(k)-2\tilde{P}_1(k-1)+\tilde{P}_1(k-2)) \quad (5)$$

where $\tilde{P}_1(k)=P_{1d}(k)-P_1(k)$ is the control error between the desired Pressure $P_{1d}(k)$ and the real Pressure $P_1(k)$, K_p it is known as the proportional gain, K_I is the integral gain and finally K_D .

To obtain better results in the PID controller, a saturation of the errors was added $y(k)=f(w,k_1,\tilde{P}_1(k))$, it is shown in the following equation (6).

$$y(k)=\left(\frac{w}{k_1+|\tilde{P}_1(k)|}\right) \quad (6)$$

This function allows to reduce large changes in the controller values that are produced by large variations in $P_{1d}(k)$.

E. The Self Tuning PID controller for Q_s

Due to the high non-linearity, parametric changes and external disturbances that occur in the dense phase system, becomes a complex system to control. In this sense the design of a self tuning PID is really necessary, because it is able to adapt the parameters of its controller in each sample time, it achieved a better performance even when there are changes in the system.

Therefore it is important to define this type of controllers in a general way, where the general discrete transfer functions of a system is given by the following equations:

$$G_p(z) = \frac{B(z^{-1})}{A(z^{-1})} \quad (7)$$

where:

$$A(z^{-1}) = 1 + a_1 z^{-1} + a_2 z^{-2}$$

$$B(z^{-1}) = b_1 z^{-1} + b_2 z^{-2}$$

The general transfer function of a controller is (8)

$$G_r(z) = \frac{Q(z^{-1})}{P(z^{-1})} \quad (8)$$

$$P(z^{-1}) = 1 + (\gamma - 1)z^{-1} - \gamma z^{-2}$$

$$Q(z^{-1}) = q_0 + q_1 z^{-1} + q_2 z^{-2}$$

Further, the following relation can be obtained for the control transfer function in closed loop

$$G(z) = \frac{B(z^{-1})Q(z^{-1})}{A(z^{-1})P(z^{-1}) + B(z^{-1})Q(z^{-1})} \quad (9)$$

where the denominator of the equation (8) is known as the characteristic polynomial. In this sense pole placement method is used for this controllers based on desired a characteristic polynomial (10) that allows the close loop transfer function stable and capable to follow a desired set point [11].The polynomial $D(z^{-1})$ can be specified by different methods. Most frequently $D(z^{-1})$, is described by the dominant poles[12].

$$D(z^{-1}) = 1 \sum_{i=0}^{n_d} d_i z^{-i} \quad (10)$$

$$A(z^{-1})P(z^{-1}) + B(z^{-1})Q(z^{-1}) = D(z^{-1})$$

$$\begin{bmatrix} b_1 & 0 & 0 & 1 & q_0 & d_1+1-a_1 \\ b_2 & b_1 & 0 & a_1-1 & q_1 & d_2+a_1-a_2 \\ 0 & b_2 & b_1 & a_2-a_1 & q_2 & a_2 \\ 0 & 0 & b_2 & a_2 & \gamma & 0 \end{bmatrix} \quad (11)$$

The equation (11) is the matrix representation of matching the desired characteristic polynomial (10) and the denominator of equation (9), finally the following compact representation is obtained

$$\mathbf{T} \mathbf{q} = \mathbf{D} \quad (12)$$

where $\mathbf{q} = [q_0 \ q_1 \ q_2 \ \gamma]$ is a vector of controller parameters uses in the equation (13)

$$A_v(k) = q_0 \tilde{Q}_s(k) + q_1 \tilde{Q}_s(k-1) + q_2 \tilde{Q}_s(k-2) \dots$$

$$\dots + (1 - \gamma) A_v(k-1) + \gamma A_v(k-2) \quad (13)$$

where $\tilde{Q}_s(k) = Q_{sd}(k) - Q_s(k)$ is the control error between the desired flow rate $Q_{sd}(k)$ and the flow of the system $Q_s(k)$, to obtain better results in this controller, a saturation of the errors was added (6). For implement this controller (13) is necessary to use recursive identification methods to estimates the system parameters $[a_1 \ a_2 \ b_1 \ b_2]$ in each sample time to get the controller parameters $\mathbf{q} = [q_0 \ q_1 \ q_2 \ \gamma]$.

One of the most popular identification algorithms is recursive least squares programming method [12] which is given by the following equations (7), (8), where $\hat{\Theta}(k) = [\hat{a}_1 \ \hat{a}_2 \ \hat{b}_1 \ \hat{b}_2]$ is the vector of estimation parameters which is updated according to the recursive relation (15)

$$\hat{\Theta}(k) = \hat{\Theta}(k-1) + \frac{\mathbf{C}(k) \phi(k-1)}{1 + \xi(k)} \hat{e}(k) \quad (14)$$

$$\xi(k) = \phi(k-1)^T \mathbf{C}(k) \phi(k-1) \quad (15)$$

$$\hat{e}(k) = Q_s(k) - \hat{\Theta}^T(k-1) \phi(k-1) \quad (16)$$

where $\xi(k)$ is an auxiliary scalar, $\hat{e}(k)$ is a prediction error and $\phi(k) = [Q_s(k-1) \ Q_s(k-2) \ A_v(k-1) \ A_v(k-2)]$ is a vector of previous values of the system. The equation (18) is the recursive relation of the covariance matrix $\mathbf{C}(k)$, $\varphi(k)$ is an exponential forgetting factor and finally $\varepsilon(k)$, $\eta(k)$, $\lambda(k)$ and $v(k)$ are auxiliary variables.

$$\mathbf{C}(k) = \mathbf{C}(k-1) - \frac{\mathbf{C}(k-1) \phi(k-1) \phi^T(k-1) \mathbf{C}(k-1)}{\varepsilon^{-1}(k) + \xi(k-1)} \quad (17)$$

$$\varepsilon(k) = \varphi(k) - \frac{1 - \varphi(k)}{\xi(k-1)} \quad (18)$$

$$\varphi(k)^{-1} = 1 + (1 + \rho)(\ln(1 + \xi(k))) \dots \quad (19)$$

$$\dots + \left(\frac{(v(k)+1) \eta(k)}{1 + \xi(k) + \eta(k)} - 1 \right) \frac{(\xi(k))}{1 + \xi(k)} \quad (20)$$

$$\eta(k) = \frac{\hat{e}^2(k)}{\lambda(k)} \quad (21)$$

$$v(k) = \varphi(k)(v(k-1)+1) \quad (22)$$

$$\lambda(k) = \varphi(k)(\lambda(k-1) + \frac{\hat{e}^2(k)}{1 + \xi(k)}) \quad (23)$$

IV. RESULTS AND DISCUSSIONS

The simulations consist of testing the proposed controller in this paper Self-Tuning PID comparing it with a classic PID tuned through experimental methods, the objective of this section is that Q_s follows a Q_{sd} while P_1 tracking P_{1d} in order to generate the slugs in respective material.

The Table 3 shows the parameters of the Self-Tuning PID controller that command the valve A_v and the parameter for de PID controller that command N .

TABLE III
PARAMETERS OF THE PROPOSED CONTROLLER

Parameters	Values	Parameters	Values
K_P	8.35	k_1	1.13
K_I	2.21	$C(k)$	$diag(1 \ 1 \ 1 \ 1)10^3$
K_D	-0.88	$\varphi(0)$	1
w	1	$\lambda(0)$	0.001
ρ	0.99	$v(0)$	0.003

F. Experiment 1

Consist of following the desired flow rate while the desired pressure remains constant. The desired values are shows in the Table 4.

TABLE IV
DESIRED VALUES OF EXPERIMENT 1

Parameters	Values
$Q_{sd}(t(k))$	50 if $t(k) \leq 40$ 75 if $40 < t(k) \leq 80$ 100 if $80 < t(k) \leq 100$ $100 + 10\sin(t(k))$ if $t(k) \geq 100$
$P_{1d}(k)$	6

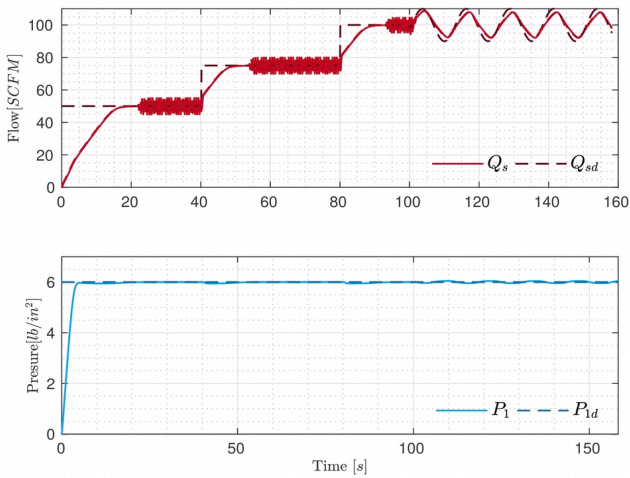


Fig. 5 Evolution of the system using Classical PID experiment 1.

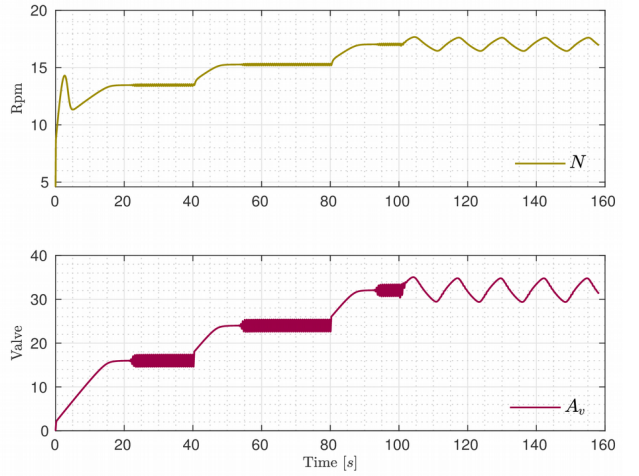
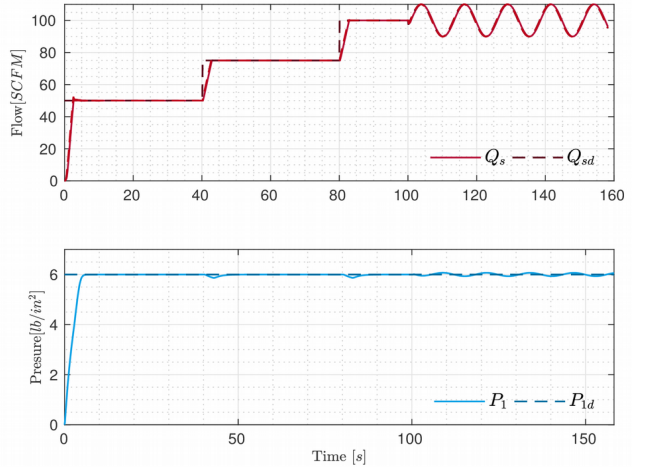


Fig. 6 Control values using Classical PID in Experiment 1.

Fig. 5 shows the evolution of the system applying Classical PID and it is appreciate that the pressure 1 tend to desired pressure but the flow rate follows the desired flow but with oscillations in steady state, which is a product of the non-linearity of the system.

Fig. 6 shows the control values applying Classical PID and it is clearly to see, that this signal present oscillations that do not allow the system to have a small control error



1. Fig. 7 Evolution of the system using Self-Tuning PID experiment 1.

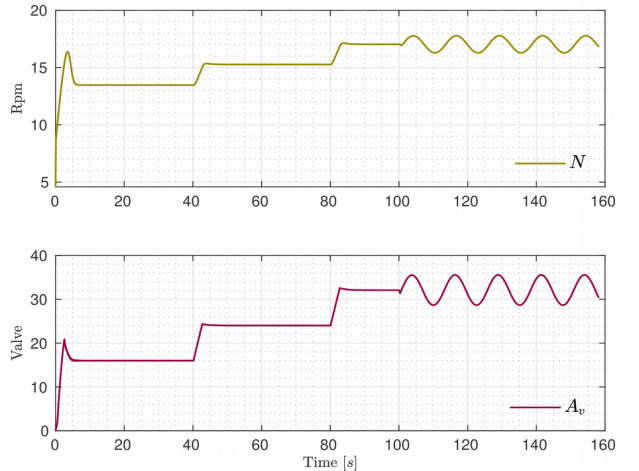


Fig. 8 Control values using Self-Tuning PID in Experiment 1.

Fig. 7 shows the evolution of the system applying Self-Tuning PID and it is appreciate that the flow rate of the system track the desired flow while the pressure 1 tends to desired pressure.

Fig. 8 shows Self-Tuning PID control values applied to the system during experiment. It is clear to see that the controller generates the appropriate control signals guaranteeing the convergence of flow rate and pressure to the desired values,

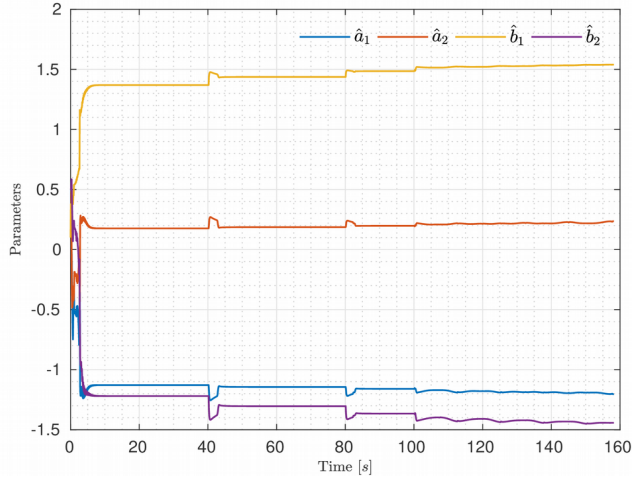


Fig. 9 Evolution of estimation parameters in experiment 1.

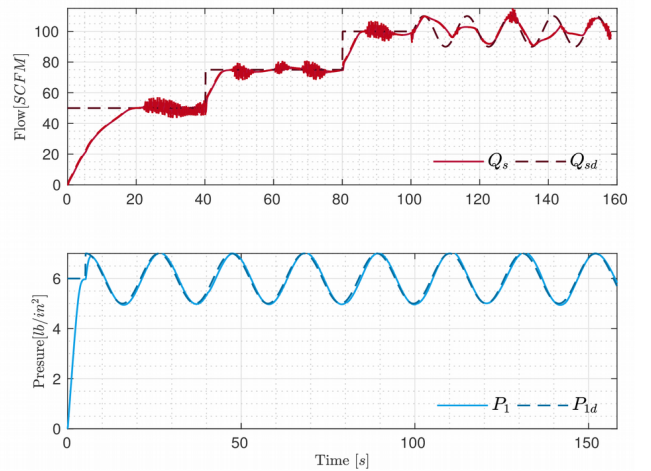
Fig. 9 shows the evolution of the estimation parameters that adapt over time in order to the control error tends to zero.

G. Experiment 2

Consist of following the desired flow rate while the desired pressure changes in the time, the desired values are shows in the Table 5.

TABLE V
PARAMETERS OF THE PROPOSED CONTROLLER

Parameters	Values
$Q_{sd}(t(k))$	50 if $t(k) \leq 40$ 75 if $40 < t(k) \leq 80$ 100 if $80 < t(k) \leq 100$ $100 + 10\sin(t(k))$ if $t(k) \geq 100$
$P_{1d}(k)$	$6 + 2\sin(t(k))$



2. Fig. 10 Evolution of the system using Self-Tuning PID experiment 2.

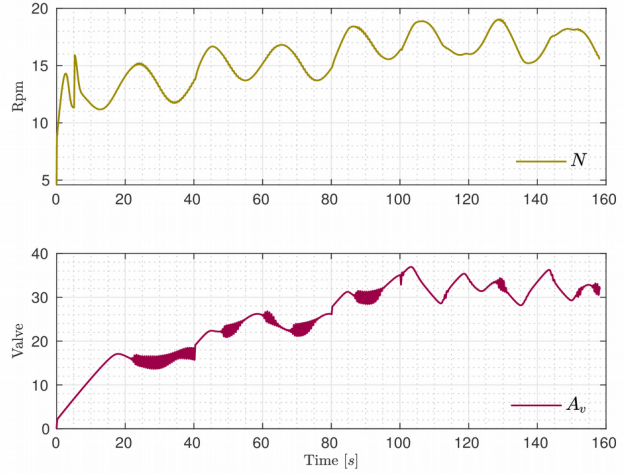
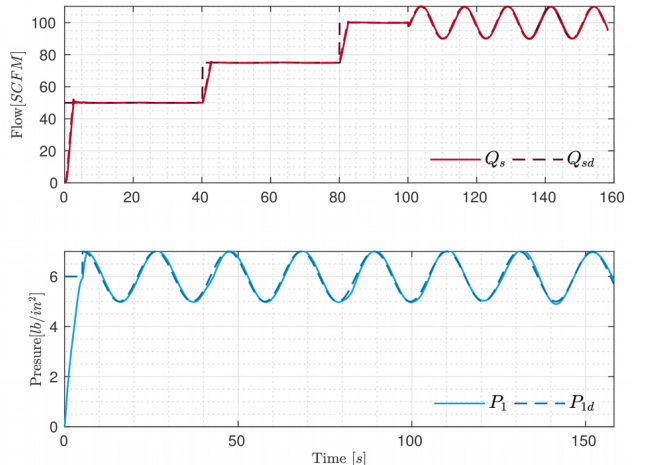


Fig. 11 Control values using Classical PID in Experiment 2.

Fig. 10 shows the evolution of the system applying Classical PID and it is appreciate that the pressure 1 tend to desired pressure but the flow rate does not tend to the desired flow, this is because the desired pressure changes cause parametric changes in the system

Fig. 11 shows the control values applying Classical PID and these signals do not allow the convergence of control errors to zero.



- ### 3. Fig. 12 Evolution of the system using Self-Tuning PID experiment 2.

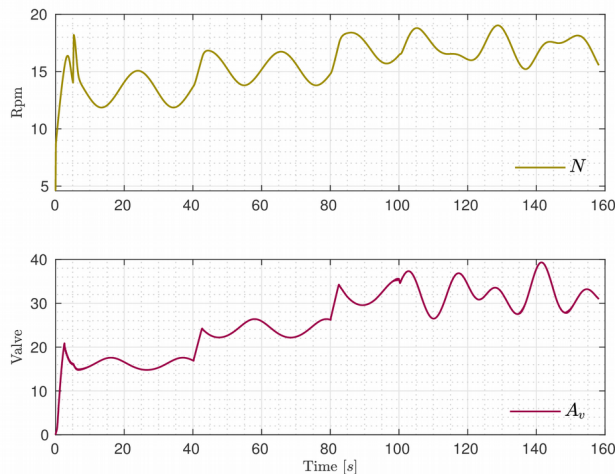


Fig. 13 Control values using Self-Tuning PID in Experiment 2.

Fig. 7 shows the evolution of the system applying Self-Tuning PID and it is appreciate that the flow rate of the system track the desired flow while the pressure 1 tends to desired pressure that changes in the time.

Fig. 8 shows Self-Tuning PID control values applied to the system during experiment. It is clear to see that the controller generates the appropriate control signals guaranteeing the convergence of flow rate and pressure to the desired values.

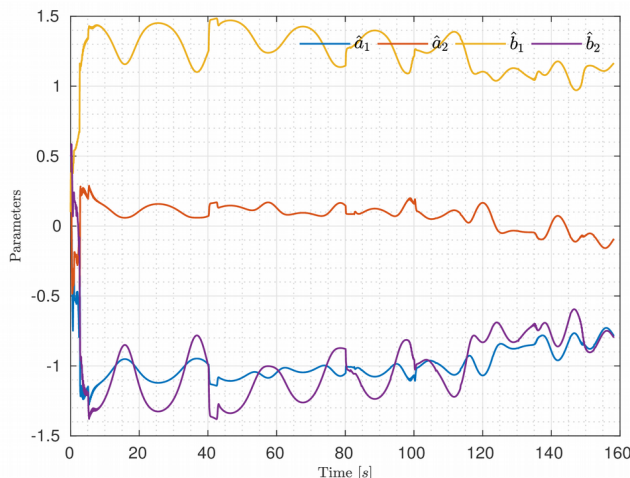


Fig. 14 Evolution of estimation parameters in experiment 2.

Fig. 14 shows the evolution of the estimation parameters that adapt over time in experiment 2 in order to the control error tends to zero.

V. CONCLUSIONS

Poner las conclusiones del trabajo bla bla
blaaaaaaaaaaaaaaaaaaaaaaaaaaaaaaaaaaaa

a
a
a
a
aa

aa
a
a
aa
a
a
a

a
a
a
a

REFERENCES

- [1] D. Neuffer, A. Alvarez, and S. Luke, “Control of Pneumatic Conveying Using ECT,” undefined, 1999.
 - [2] D. Mills, “Chapter 1 - Introduction to Pneumatic Conveying and the Guide,” in Pneumatic Conveying Design Guide (Third Edition), Third Edit., D. Mills, Ed. Butterworth-Heinemann, 2016, pp. 3–32.
 - [3] G. E. Klinzing, F. Rizk, R. Marcus, and L. S. Leung, “An Overview of High-Pressure Systems Including Long-Distance and Dense Phase Pneumatic Conveying Systems,” 2010, pp. 331–355
 - [4] D. Mills, “Chapter 4 - Applications and Capabilities,” in Pneumatic Conveying Design Guide (Third Edition), Third Edit., D. Mills, Ed. Butterworth-Heinemann, 2016, pp. 81–100.
 - [5] W. Chen, K. C. Williams, and M. G. Jones, “Chapter 23 - Applications of Numerical Modeling in Pneumatic Conveying,” in Pneumatic Conveying Design Guide (Third Edition), Third Edit., D. Mills, Ed. Butterworth-Heinemann, 2016, pp. 521–552.
 - [6] K. K. Tan, R. Ferdous, and S. Huang, “Closed-loop automatic tuning of PID controller for nonlinear systems,” Chem. Eng. Sci., vol. 57, no. 15, pp. 3005–3011, 2002, doi: [https://doi.org/10.1016/S0009-2509\(02\)00186-0](https://doi.org/10.1016/S0009-2509(02)00186-0).
 - [7] S. D. Sahputro, F. Fadilah, N. A. Wicaksono, and F. Yusivar, “Design and implementation of adaptive PID controller for speed control of DC motor,” in QiR 2017 - 2017 15th International Conference on Quality in Research (QIR): International Symposium on Electrical and Computer Engineering, Dec. 2017, vol. 2017-December, pp. 179–183, doi: 10.1109/QIR.2017.8168478.
 - [8] “Handbook - Education - CAGI - Compressed Air And Gas Institute.” <https://www.cagi.org/education/handbook.aspx> (accessed Nov. 10, 2020).
 - [9] L. F. Recalde, B. S. Guevara, G. Cuzco, and V. H. Andaluz, “Optimal control problem of a differential drive robot,” in Lecture Notes in Computer Science (including subseries Lecture Notes in Artificial Intelligence and Lecture Notes in Bioinformatics), Sep. 2020, vol. 12144 LNAI, pp. 75–82, doi: 10.1007/978-3-030-55789-8_7.
 - [10] R. Hernández-Alvarado, L. García-Valdovinos, T. Salgado-Jiménez, A. Gómez-Espinoza, and F. Fonseca-Navarro, “Neural Network-Based Self-Tuning PID Control for Underwater Vehicles,” Sensors, vol. 16, no. 9, p. 1429, Sep. 2016, doi: 10.3390/s16091429.
 - [11] A. S. Hauksdóttir and S. Sigurðsson, “A Pole Placing PID Type Controller,” IFAC-PapersOnLine, vol. 51, no. 4, pp. 942–947, Jan. 2018, doi: 10.1016/j.ifacol.2018.06.101.
 - [12] M. Manyari-Rivera and J. Basilio, “Integrated online auto-tuning and digital implementation of PID controllers in industrial processes,” in IEEE International Conference on Control and Automation, ICCA, 2011, pp. 550–555, doi: 10.1109/ICCA.2011.6137985.

